

## Articles

# Enzyme-Amplified Electrochemical Detection of DNA Using Electrocatalysis of Ferrocenyl-Tethered Dendrimer

Eunkyung Kim,<sup>†</sup> Kyuwon Kim,<sup>‡</sup> Haesik Yang,<sup>\*,‡</sup> Youn Tae Kim,<sup>‡</sup> and Juhyoun Kwak<sup>\*,†</sup>

Department of Chemistry, Korea Advanced Institute of Science and Technology (KAIST), Daejeon 305-701, Republic of Korea, and BioMEMS Team, Electronics and Telecommunications Research Institute (ETRI), Daejeon 305-600, Republic of Korea

**We have developed a sandwich-type enzyme-linked DNA sensor as a new electrochemical method to detect DNA hybridization. A partially ferrocenyl-tethered poly(amido-amine) dendrimer (Fc-D) was used as an electrocatalyst to enhance the electronic signals of DNA detection as well as a building block to immobilize capture probes. Fc-D was immobilized on a carboxylic acid-terminated self-assembled monolayer (SAM) by covalent coupling of unreacted amine in Fc-D to the acid. Thiolated capture probe was attached to the remaining amine groups of Fc-D on the SAM via a bifunctional linker. The target DNA was hybridized with the capture probe, and an extension in the DNA of the target was then hybridized with a biotinylated detection probe. Avidin-conjugated alkaline phosphatase was bound to the detection probe and allowed to generate the electroactive label, *p*-aminophenol, from *p*-aminophenyl phosphate enzymatically. *p*-Aminophenol diffuses into the Fc-D layer and is then electrocatalytically oxidized by the electronic mediation of the immobilized Fc-D, which leads to a great enhancement in signal. Consequently, the amount of hybridized target can be estimated using the intensity of electrocatalytic current. This DNA sensor exhibits a detection limit of 20 fmol. Our method was also successfully applied to the sequence-selective discrimination between perfectly matched and single-base mismatched target oligonucleotides.**

The DNA microarray approach has become increasingly important in basic research into the genetics of disease and also in the more practical applications of medical diagnosis and treatment. Various methods have been used to detect sequence-selective DNA hybridization, including optical,<sup>1,2</sup> electrochemical,<sup>3–19</sup>

and piezoelectric transduction techniques.<sup>20,21</sup> Of these techniques, the electrochemical method has attracted particular attention because of its high sensitivity, low cost, and compatibility with microfabrication technology. The recent developments of electrochemical DNA biosensor have been reviewed in several reports.<sup>3–6</sup>

Korri-Youssoufi et al. developed a method for direct, label-free, electrical DNA detection. In this approach, the electrical signal is monitored by changes in the conductivity of conducting polymer molecular interfaces, for example, using DNA-substituted or -doped polypyrrole films.<sup>7</sup> Thorp's group has developed a method for the detection of nucleic acids based on the electrochemical oxidation of guanine in target DNA with the mediator Ru(bpy)<sub>3</sub><sup>3+</sup>,

\* Corresponding authors. E-mails: (J. Kwak) jhkwa@kaist.ac.kr; (H. Yang) hsyang@etri.re.kr.

<sup>†</sup> KAIST.

<sup>‡</sup> ETRI.

- (1) Piuono, P. A. E.; Krull, U. J.; Hudson, R. H. E.; Damha, M. J.; Cohen, H. *Anal. Chem.* **1995**, *67*, 2635.
- (2) Jenison, R.; Yang, S.; Haeblerli, A.; Polisky, B. *Nat. Biotechnol.* **2001**, *19*, 62.
- (3) Wang, J. *Anal. Chim. Acta* **2002**, *469*, 63.
- (4) Palecek, E.; Fojta, M. *Anal. Chem.* **2001**, *73*, 75A.

- (5) Wang, J. *Chem. Eur. J.* **1999**, *5*, 1681.
- (6) Popovich, N. D.; Thorp, H. H. *Interface* **2002**, 30.
- (7) Korri-Youssoufi, H.; Garnier, F.; Srivastava, P.; Godillot, P.; Yassar, A. *J. Am. Chem. Soc.* **1997**, *119*, 7388.
- (8) Napier, M. E.; Loomis, C. R.; Sistare, M. F.; Kim, J.; Eckhardt, A. E.; Thorp, H. H. *Bioconjugate Chem.* **1997**, *8*, 906.
- (9) Wang, J.; Rivas, G.; Fernandes, J. R.; Paz, J. L. L.; Jiang, M.; Waymire, R. *Anal. Chim. Acta* **1998**, *375*, 197.
- (10) Jelen, F.; Yosypchuk, B.; Kourilova, A.; Novotny, L.; Palecek, E. *Anal. Chem.* **2002**, *74*, 4788.
- (11) Palecek, E.; Billova, S.; Havran, L.; Kizek, R.; Miculikova, A.; Jelen, F. *Talanta* **2002**, *56*, 919.
- (12) Millan, K. M.; Mikkelsen, S. R. *Anal. Chem.* **1993**, *65*, 2317.
- (13) Millan, K. M.; Sarullo, A.; Mikkelsen, S. R. *Anal. Chem.* **1994**, *66*, 2943.
- (14) Boon, E. M.; Ceres, D. M.; Drummond, T. G.; Hill, M. G.; Barton, J. K. *Nat. Biotechnol.* **2000**, *18*, 1096.
- (15) Takenaka, S.; Yamashita, K.; Takagi, M.; Uto, Y.; Kondo, H. *Anal. Chem.* **2000**, *72*, 1334.
- (16) Yu, C. J.; Wan, Y.; Yowanto, H.; Li, J.; Tao, C.; James, M. D.; Tan, C. L.; Blackburn, G. F.; Meade, T. J. *J. Am. Chem. Soc.* **2001**, *123*, 11155.
- (17) (a) Patolsky, F.; Lichtenstein, A.; Willner, I. *Nat. Biotechnol.* **2001**, *19*, 253. (b) Patolsky, F.; Katz, E.; Bardea, A.; Willner, I. *Langmuir* **1999**, *15*, 3703. (c) Patolsky, F.; Lichtenstein, A.; Willner, I. *Angew. Chem., Int. Ed.* **2000**, *39*, 940.
- (18) (a) Campbell, C. N.; Gal, D.; Cristler, N.; Banditrat, C.; Heller, A. *Anal. Chem.* **2002**, *74*, 158. (b) Caruana, D. J.; Heller, A. *J. Am. Chem. Soc.* **1999**, *121*, 769. (c) Dequaire, M.; Heller, A. *Anal. Chem.* **2002**, *74*, 4370. (d) Zhang, Y.; Kim, H.-H.; Mano, N.; Dequaire, M.; Heller, A. *Anal. Bioanal. Chem.* **2002**, *374*, 1050.
- (19) Palecek, E.; Kizek, R.; Havran, L.; Billova, S.; Fojta, M. *Anal. Chim. Acta* **2002**, *469*, 73.
- (20) Caruso, F.; Rodda, E.; Furlong, D. N.; Niikura, K.; Okahata, Y. *Anal. Chem.* **1997**, *69*, 2043.
- (21) Bardea, A.; Dagan, A.; Ben-Dov, I.; Amit, B.; Willner, I. *Chem. Commun.* **1998**, 839.

which enables the detection of PCR-amplified genomic DNA.<sup>8</sup> Wang et al. demonstrated that potentiometric stripping analysis can be used to directly monitor guanine oxidation in target DNA.<sup>9</sup> Recently, Jelen et al. have developed a new method using a dual-electrode system in which the hybridization is performed at one surface and the electrochemical detection of adenine at another surface by cathodic stripping voltammetry.<sup>10,11</sup> In this technique, the nonspecific adsorption of DNA at the electrode is negligible, which makes it possible to detect hybridization of longer target DNA with great sensitivity and specificity. Such methods have the advantage that the modification of target oligonucleotide is not required, but do present difficulties with quantification, because the electric signal is dependent on the number of guanine residues within the target oligonucleotides.

Electrochemical DNA detection methods using various labels have also been developed. A number of studies have shown that electroactive intercalators can detect selective hybridization when combined with electrochemical measurements.<sup>12–15</sup> Since these intercalators bind to single-stranded DNA as well as to double helix DNA (by means of the electrostatic interaction with the phosphate groups of the DNA backbone), this method may produce high background currents. To improve the detection sensitivity, a number of studies have attempted to use label-conjugated oligonucleotides. Yu et al. electronically detected single-base mismatches in DNA with ferrocene-modified probes in which ferrocenyl derivatives are inserted at various positions on oligonucleotide probes using automated DNA/RNA synthesis techniques.<sup>16</sup> Recently, Willner et al. used faradaic impedance spectroscopy as a powerful tool for the detection of sequence-selective DNA hybridization and demonstrated that enzyme labels, such as peroxidase and alkaline phosphatase, induce the biocatalyzed precipitation on electronic transducers and amplification of signal.<sup>17</sup> They showed that the method is capable of detecting 10 pM mutant DNA.<sup>17a</sup> Enzyme labels have also been used by Heller et al., who reported that a 38-base oligonucleotide can be detected at 20 pM in an electrochemical enzyme-amplified sandwich-type assay.<sup>18d</sup> In their system, the redox polymer-modified electrode is electronically coupled to the redox centers of peroxidase enzymes that electrocatalyze the reduction of hydrogen peroxide to water. The amount of electrocatalyzed current indicates the degree of hybridization of target DNA with surface-bound DNA.<sup>18</sup> In another approach, some attempts have been made to apply the previous technique in the electrochemical enzyme immunoassay to a DNA biosensor,<sup>19,27,28</sup> which is a very important point in this paper.

Dendritic nucleic acids were previously used in order to enhance the sensitivity of DNA biosensors because of their

hyperbranched spherical structure.<sup>22,23</sup> In this study, partially ferrocenyl-tethered dendrimers have been used as a building block and an electrocatalyst in a new electrochemical DNA sensor. The initial layer of our DNA sensor assembly is covered with Fc-D on the acid-terminated self-assembled monolayer (SAM). The thiolated capture probes are then covalently immobilized via bifunctional linkers on the remaining amine groups of Fc-D. Compared to conventional surfaces with linear chemical linkers,<sup>24</sup> the dendrimer-activated surfaces have a 2-fold greater capacity to immobilize oligomers. Next, the resulting assembly is hybridized with the target, followed by biotinylated detection probes. We adopted a sandwich-type method for detecting DNA or RNA<sup>25</sup> in which the target is hybridized to the immobilized capture probe and then hybridized with a label-conjugated detection probe, because this approach avoids the need to modify the target. The biotin label on the detection probes also has the advantages of being thermally stable under melting conditions and being able to bind with various avidin-conjugated enzymes, which might be useful in the application of multiple labels. Last, the biotin-terminated layer is detected using avidin-conjugated alkaline phosphatase (Av-ALP), which generates the electroactive species *p*-aminophenol (*p*-AP) from its substrate *p*-aminophenyl phosphate (*p*-APP). This approach has been used in an electrochemical enzyme immunoassay (EEIA)<sup>26</sup> in which the enzymatic properties of ALP provide amplification, leading to higher sensitivity.<sup>26a</sup> Our use of ALP as an electroactive label generator contrasts with approaches that have used this enzyme to precipitate reaction products on electrodes and detect them using optical or faradaic impedance spectroscopic methods.<sup>2,17</sup> Finally, *p*-AP diffuses onto the immobilized Fc-D layer, where it is electrocatalytically oxidized with the mediation of the ferrocene in the layer. To our knowledge, no previous studies on the EEIA method have reported the enhancement of electrochemical signals from the enzymatic products using electrocatalysis in an electroactive layer of a DNA sensor.<sup>19,27,28</sup> In this approach, the generation of the electroactive label, *p*-AP, is amplified by enzymatic reaction of ALP, and the electric signal of its electrochemical oxidation is enhanced by electronic mediation of Fc-D. The electrocatalytic current is monitored as an indicator of the hybridization of DNA using cyclic voltammetry (CV). In this study, we characterized the construction of a sandwich-type electrochemical DNA sensor with FT-IR, investigated its electrochemical properties with CV, and compared the electrochemical results with those obtained from surface plasmon resonance (SPR) spectroscopy experiments. Furthermore, we investigated whether our technique enables not only the detection of sequence-selective hybridization involving a single-base mismatched target but also the quantification of target oligonucleotides.

## EXPERIMENTAL SECTION

**Chemicals and Reagents.** Amine-terminated G4 poly(amidoamine) (PAMAM) dendrimer, ferrocenecarboxaldehyde, and sodium borohydride were purchased from Aldrich. 1-Ethyl-3-[3-(dimethylamino)propyl]carbodiimide hydrochloride (EDC), and *N*-hydroxysuccinimide (NHS) were obtained from Sigma. All buffer salts and other inorganic chemicals were obtained from Sigma or Aldrich unless otherwise stated. All chemicals were used as received. Ultrapure water (>18 M $\Omega$ ) from a Modulab water system (U.S. Filter Corp.) was used throughout this work.

(22) Wang, J.; Jiang, M.; Nilsen, T. W.; Getts, R. C. *J. Am. Chem. Soc.* **1998**, *120*, 8281.

(23) Wang, J.; Rivas, G.; Fernandes, J. R.; Jiang, M.; Paz, J. L. L.; Waymire, R.; Nielsen, T. W.; Getts, R. C. *Electroanalysis* **1998**, *10*, 553.

(24) Benters, R.; Niemeyer, C. M.; Wöhrle, D. *ChemBioChem* **2001**, *2*, 686.

(25) Huang, T. J.; Liu, M.; Knight, L. D.; Grody, W. W.; Miller, J. F.; Ho, C.-M. *Nucleic Acids Res.* **2002**, *30*, e55.

(26) (a) Thompson, R. Q.; Barone, G. C., III; Halsall, H. B.; Heineman, W. R. *Anal. Biochem.* **1991**, *192*, 90. (b) Limoges, B.; Degrand, C. *Anal. Chem.* **1996**, *68*, 4141. (c) Santandreu, M.; Céspedes, F.; Alegret, S.; Martínez-Fàbregas, E. *Anal. Chem.* **1997**, *69*, 2080.

(27) Bagel, O.; Degrand, C.; Limoges, B.; Joannes, M.; Azek, F.; Brossier, P. *Electroanalysis* **2000**, *12*, 1447.

(28) Xu, D.; Huang, K.; Liu, Z.; Liu, Y.; Ma, L. *Electroanalysis* **2001**, *13*, 882.

Table 1. Sequence of Modified Oligonucleotide Strands

oligonucleotide	sequence (5' → 3')
capture probe (C)	GTA AAA CGA CGG CCA G
detection probe (D)	TTA TAA CTA TTC CTA TTT TT
target (T1)	TAG GAA TAG TTA TAA CTG GCC GTC GTT TTA C
target (T2)	TAG GAA TAG TTA TAA AAA GCT GAC CAG ACA G
target (T3)	TAG GAA TAG TTA TAA CTG GCC GTC GTC TTA C

*p*-Aminophenyl phosphate monohydrated (*p*-APP) was purchased from Universal Sensors (Cork, Ireland). Neutravidin-conjugated alkaline phosphatase (Av-ALP) and succinimidyl 4-(*N*-maleimidomethyl)cyclohexane-1-carboxylate (SMCC) were obtained from Pierce (Rockford, IL).

The hybridization buffer (HB) consisted of 20 mM tris-(hydroxymethyl)aminomethane hydrochloride (Tris), 5 mM ethylenediaminetetraacetic acid, 150 mM NaCl, and 0.05% Tween 20 (pH 7.4). The dehybridization buffer (DHB) was composed of 0.3 mM NaCl, 30 mM Tris, and 0.1% sodium dodecyl sulfate (pH 7.4). The binding buffer (BB) for associating with Av-ALP consisted of 50 mM Tris, 0.3 M NaCl, 0.5% Tween 20, and 1% bovine serum albumin (pH 7.4). The rinsing buffer (RB) was 50 mM Tris, 0.5 M NaCl, and 0.05% Tween 20 (pH 7.4). The buffer (EB) for the electrochemical experiment used was 50 mM Tris, 10 mM KCl, and 1 g/L MgCl<sub>2</sub> (pH 9.0).

All oligonucleotides employed in this work were synthesized and purified using an HPLC apparatus supplied by GenoTech (Daejeon, Korea). Capture probes were modified with 5'-thiol-terminated 6-carbon spacers (-(CH<sub>2</sub>)<sub>6</sub>-). A 9-atom ethylene glycol linker group (-(C<sub>2</sub>H<sub>4</sub>O)<sub>3</sub>-) was appended on the 5' end of a capture probe to improve hybridization efficiency and prevent nonspecific binding of proteins. The detection probe (D) was 3'-labeled with a biotin group, and a 5-T (thymine) spacer was inserted between the oligomer and the biotin. The targets for the sandwich hybridization (T1, T2, and T3) were designed using complementary, noncomplementary, and single-base-mismatched oligonucleotides, respectively, as shown in Table 1.

**Preparation of Partially Ferrocenyl-Tethered PAMAM G4 Dendrimer (Fc-D).** Partially ferrocenyl-tethered PAMAM dendrimer was synthesized by an imine formation reaction between partial primary amines of NH<sub>2</sub>-terminated G4 PAMAM dendrimer and ferrocenecarboxaldehyde, as previously described.<sup>29,31</sup> Ferrocenecarboxaldehyde (22.5 mg) was dissolved in 10 mL of methanol, and the mixture was added dropwise to 0.75 mL of 10% (w/w) G4 PAMAM dendrimer solution containing hydrochloric acid as a catalyst. The reaction mixture was slowly stirred for 2 h. A solution of sodium borohydride (15 mg in 10 mL of methanol) was slowly added, and the resulting solution was stirred for 1 h to reduce carbon-to-nitrogen double bonds. The reaction product was purified by lipophilic gel permeation chromatography (Sephadex LH-20, Pharmacia) using methanol as the eluant. On the basis of previous studies,<sup>29</sup> the extent of primary amine modification was estimated to be 30%.

**Quantification of Immobilized Capture Probe and Hybridized Target by Autoradiography.** To quantify the surface density

of capture probes attached on the Fc-D-modified electrode, the 3' end of the capture probe was labeled with [ $\alpha$ -<sup>32</sup>P]ddATP (Amersham, Piscataway, NJ) using terminal transferase (Promega, USA). The probes electrostatically adsorbed on the Fc-D-modified electrode were washed out twice with RB and dried with nitrogen gas. The surface density of the hybridized target was measured using 5'-<sup>32</sup>P-labeled complementary target oligomer that had been radiolabeled using T4 polynucleotide kinase (Promega, USA) and [ $\gamma$ -<sup>32</sup>P]ATP from IZOTOP (Institute of Isotope Co. Inc.). Quantification was performed from radioimages using a Fuji Bio-Imaging Analyzer model Bas 2000.

**Construction of Sandwich-Type Enzyme-Linked Electrochemical DNA Sensor.** Gold electrodes were prepared by electron-beam evaporation of 40 nm of Ti followed by 150 nm of Au onto Si (100) wafers. The electrode was cleaned in piranha solution (30% H<sub>2</sub>O<sub>2</sub>/70% H<sub>2</sub>SO<sub>4</sub>), rinsed with water, and then dried with nitrogen gas. (WARNING: piranha reacts violently with organics.) The clean electrode was immersed in a mixed solution of mercaptododecanoic acid (MDA) and mercaptoundecanol (MUO) (1 mM:4 mM) for 12 h, washed with pure ethanol, and dried with N<sub>2</sub> gas. The carboxylic groups were activated by immersion of the electrode into a mixed solution of 50 mM EDC and 25 mM NHS for 2 h, and the Fc-D solution (100  $\mu$ M) was spotted onto the activated electrode and left to incubate for 2 h. Electrostatically attached Fc-D was removed by rinsing twice with RB. To attach the thiolated capture probes onto the Fc-D modified electrode, the electrode was immersed into a solution containing 1 mM SMCC in *N,N*-dimethylformamide for 2 h, and then a solution containing 1  $\mu$ M capture probe was spotted onto the electrode. The hybridization step between the target and detection probe was carried out by incubation in each solution for 2 h at room temperature, followed by washing twice for 10 min with DHB at 35 °C. Before the association with Av-ALP, the electrode was prepared by immersion in BB for 30 min to prevent the nonspecific adsorption of protein. The resulting assembly was immersed in BB solution containing 8  $\mu$ L/mL Av-ALP for 5 min at 4 °C, followed by two washes in RB.

**Instruments.** The electrochemical experiment was performed using a BAS 100B (Bioanalytical Systems, Inc.). The three-electrode electrochemical cell consisted of the modified Au electrode, a Pt wire counter electrode and Hg/Hg<sub>2</sub>SO<sub>4</sub> (Mercury Sulfate Electrode: MSE, saturated K<sub>2</sub>SO<sub>4</sub>) reference electrode. The cell was filled with EB containing 0.5 mM *p*-APP and deoxygenated with Ar. The solution of *p*-APP was prepared daily.

IR spectra were acquired using a nitrogen-purged Nexus FT-IR spectrometer equipped with the Smart SAGA (Smart Apertured Grazing Angle) accessory (Thermo Nicolet, WI). Polarized light at an angle of 80° with respect to the surface normal was used.

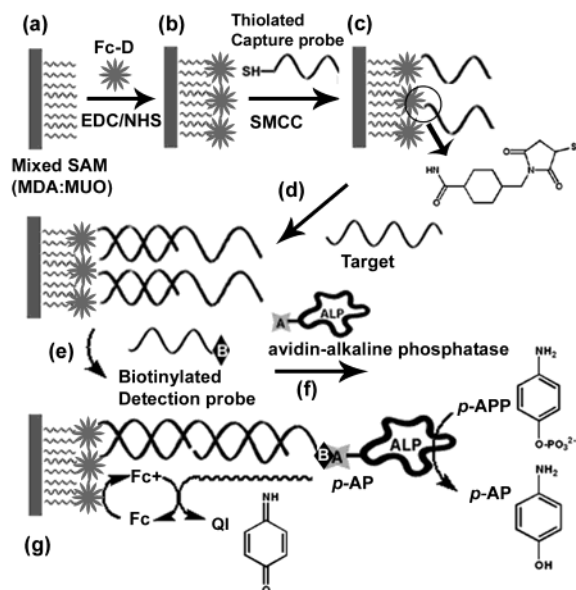
(29) Yoon, H. C.; Hong, M.-Y.; Kim, H.-S. *Anal. Chem.* **2000**, *72*, 4420.

(30) Oh, S.-K.; Baker, L. A.; Crooks, R. M. *Langmuir* **2002**, *18*, 6981.

(31) Yoon, H. C.; Hong, M.-Y.; Kim, H.-S. *Anal. Biochem.* **2000**, *282*, 121.



Scheme 1. Stepwise Assembly of a Sandwich-Type Enzyme-Linked DNA-Sensing Electrode



(a) Formation of mixed SAM on Au electrode, (b) immobilization of Fc-D, (c) immobilization of thiolated capture probe with bifunctional linker (SMCC), (d) hybridization with target, (e) hybridization with biotinylated detection probe, (f) association with avidin-alkaline phosphatase, (g) description of the process of the electrocatalytic reaction of *p*-AP via electronic mediation of Fc-D.

All spectra were reported in the absorption mode relative to a clean gold electrode.

SPR measurements were made with a BIAcore X instrument. The immobilization of Fc-D was achieved on the mixed SAM with the bare gold substrate of the sensor chip SIA Kit Au (BIAcore AB). SPR experiments were conducted with a constant 5  $\mu\text{L}/\text{min}$  flow of solution over the surfaces. The consecutive adsorption of each target, detection probe, and Av-ALP was carried out by sequential injections of 100  $\mu\text{L}$  of the 1  $\mu\text{M}$  target (T1 or T2) in HB, 100  $\mu\text{L}$  of the 1  $\mu\text{M}$  detection probe in HB, and subsequently, 35  $\mu\text{L}$  of the 8  $\mu\text{L}/\text{mL}$  Av-ALP in BB. The surface was washed with RB after each injection. Adsorption of each component resulted in a shift in the resonance angle that was reported in resonance units (RU; 10 000 RU = 1.0°).

## RESULTS AND DISCUSSION

**Construction of Sandwich-Type Enzyme-Linked Electrochemical DNA Sensor.** Scheme 1 depicts the stepwise construction process of the sandwich-type enzyme-linked electrochemical DNA sensor. First, the clean gold electrode was covered with mixed SAM (MDA/MUO (1:4)), as shown in Scheme 1a. MDA was used for immobilizing Fc-D, and MUO was utilized to prevent nonspecific binding of proteins. Additionally, since the compact mixed SAM blocks the close approach of the soluble redox reagents to the electrode, we can exclude the possibility of direct electron transfer reaction on the gold electrode. The carboxyl groups of the SAM were activated with EDC/NHS and reacted with the free amine groups of Fc-D (Scheme 1b). Although the assembly of the Fc-D layer in our DNA assay system is rather complex, it affords two important advantages. First, it provides

an efficient binding site for the covalent attachment of a thiolated capture probe on the sensor surfaces through the unreacted amine moiety of Fc-D. Second, it acts as an electrocatalyst to shuttle electrons between the electroactive products generated by enzymatic reaction and the electrode by means of a recycling redox reaction of the ferrocene component. Although these two roles of Fc-D have been demonstrated previously,<sup>29–31</sup> few studies have examined its application in DNA hybridization detection.

Subsequently, capture probes were covalently attached to the Fc-D modified surface, as described in Scheme 1c. The unmodified amine groups of immobilized Fc-D were terminated with a bifunctional linker, SMCC, which contains both NHS ester and maleimide groups. The NHS ester end of the molecule reacts with the free amine groups on the Fc-D modified surface. The surface terminated with maleimide groups binds thiolated capture probes covalently. The amount of immobilized capture probe was estimated as  $4.8 \times 10^{-12}$  ( $\pm 0.02$ ) mol/cm<sup>2</sup> by autoradiography. This value corresponds to only 30% of the surface coverage obtained by Benters et al. in a previous study on the immobilization of the capture probe on the dendrimer-activated surface.<sup>24</sup> The low coverage we obtained can be attributed to the partial modification of the amines of the dendrimers with ferrocenyl groups. As a next step, the immobilized capture probes were hybridized with target DNA (Scheme 1d) and then biotinylated detection probes needed for enzyme binding (Scheme 1e). Subsequently, Av-ALP was associated with each hybrid (Scheme 1f). If the target is complementary to the immobilized capture probe, the supplementary parts of the attached target can hybridize with the biotinylated detection probes. Av-ALP associates with the exposed biotin group and converts *p*-APP to an electroactive *p*-AP, which diffuses to near the Fc-D layer (Scheme 1g). The oxidative reaction of diffused *p*-AP is electrocatalyzed by the Fc-D, and the amount of electrocatalytic current indicates the extent of hybridization of the target oligomers.

**Characterization of Modified Surfaces Using FT-IR.** After each of the steps in Scheme 1, we characterized the modified surfaces using FT-IR. The spectrum of the mixed SAM on the electrode is shown in Figure 1a. In agreement with a previously reported spectrum of this SAM,<sup>32</sup> two prominent peaks appear in the positions of the asymmetrical and symmetrical C–H stretching modes of the methylene groups of alkyl chains at 2918 and 2849 cm<sup>-1</sup>, respectively. These peak positions strongly support the argument that these alkyl chains are in densely packed, crystalline-like environments that are quite similar to those found in long-chain thiol assemblies. The peak at 2880 cm<sup>-1</sup> might be due to a C–H stretching mode of the hydroxymethyl groups. Chidsey et al. observed a similar feature in spectra of 11-mercaptoundecanol, which is consistent with our results.<sup>33</sup> However, the C=O stretching mode of mercaptododecanoic acid is not observed in Figure 1a. It is possible that the coverage of the carbonyl group in the mixed SAM is much lower than that of the hydroxyl group.

The spectrum of the surface recorded after the immobilization of Fc-D (Figure 1b) showed three features characteristic of a PAMAM dendrimer: a broad peak at around 3300 cm<sup>-1</sup> attributed to the N–H stretching vibration and two bands at 1659 and 1552 cm<sup>-1</sup> assigned to the amide I (amide carbonyl stretch) and amide

(32) Nuzzo, R. G.; Dubois, L. H.; Allara D. L. *J. Am. Chem. Soc.* **1990**, *112*, 558.

(33) Chidsey, C. E. D.; Loiacono, D. N. *Langmuir* **1990**, *6*, 682.

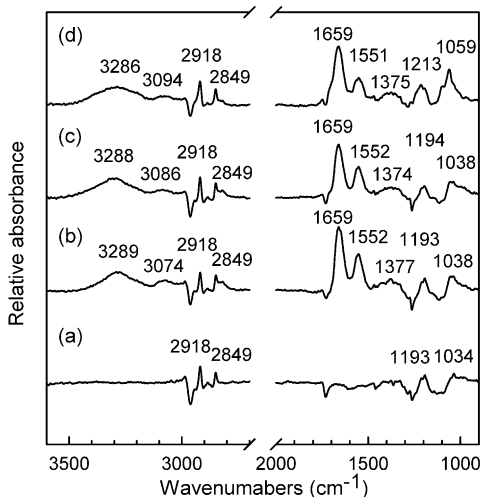


Figure 1. Spectra of the modified electrode surface after each step was carried out, as described in Scheme 1: (a) formation of mixed SAM, (b) immobilization of Fc-D, (c) activation of Fc-D surface with SMCC, and (d) immobilization of thiolated capture probe.

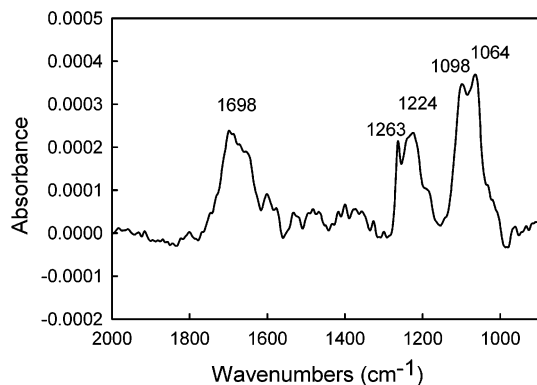


Figure 2. Spectrum showing the difference between two FT-IR spectra, one of the SMCC surface (Figure 1c) and one of the modified surfaces after adsorption of thiolated capture probe (Figure 1d).

II bands (amide C–N stretch) of Fc-D, respectively.<sup>34</sup> The small band near 3100  $\text{cm}^{-1}$  might be due to the C–H stretching absorption of the ferrocene ring of Fc-D. A similar band was previously observed in IR spectra of  $\text{FcCOOC}_{11}\text{SH}$  and  $\text{FcC}_{11}\text{SH}$  monolayer.<sup>35</sup>

Figure 2 shows the differential spectrum between the SMCC-modified electrode spectrum (Figure 1c) and the spectrum of the surface after the covalent adsorption of the thiol-terminated capture probe (Figure 1d). This difference spectrum is calculated because the bands of Fc-D are too strong to observe the spectral features due to the DNA. In Figure 2, the band at 1698  $\text{cm}^{-1}$  is due to the double-bond stretching vibrations of the DNA bases, the 1263  $\text{cm}^{-1}$  band results from an N–H bending vibration on the base thymine, and the absorption bands at 1224  $\text{cm}^{-1}$  and near 1073  $\text{cm}^{-1}$  are, respectively, the asymmetric and symmetric stretching vibration of the phosphates. The assignment of these

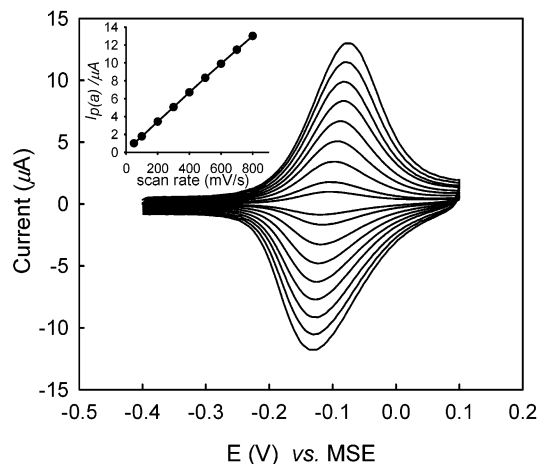


Figure 3. Cyclic voltammogram of Fc-D-modified electrode dependent on scan rate from 50–800  $\text{mV/s}$  in EB. (Inset box) Plot of anodic peak currents to potential sweep rates.

bands in Figure 2 is in accordance with previous studies on the characterization of DNA structure using FT-IR.<sup>36,37</sup> These results support the sequential assembly of mixed SAM, Fc-D, and thiolated capture probe DNA via the respective linkers described in Scheme 1.

#### Alkaline Phosphatase as an Electroactive Label Generator and Electrocatalytic Oxidation of *p*-AP at the Fc-D-Modified Electrode.

The utility of ALP as an electroactive label generator originates from EEIA, in which an antibody or antigen-labeled enzyme acts on substrates such as *p*-APP, *p*-nitrophenyl phosphate, or phenyl phosphate and biocatalytically generates a redox-active product that can be detected using electrochemical methods.<sup>26,38,39</sup> First, we investigated the electrochemical properties of the gold electrode modified with Fc-D on the mixed SAM. Figure 3 displays the typical CV features of the surface-bound molecules. The peak currents linearly increase with scan rate up to 800  $\text{mV/s}$ , and the peak separation ( $\Delta E_p$ ) between the cathodic and anodic peaks is 12 mV at a scan rate of 100  $\text{mV/s}$ . The full width at half-maximum is  $\sim 100$  mV, indicating a large formal peak separation, whereas the ideal value for reversible responses is  $90.6/n$  mV. From the cyclic voltammogram, the surface coverage of Fc-D was calculated by dividing the total coverage of ferrocene sites (obtained from the coulometric charge, which was calculated by integrating the anodic peak area in the CV of Figure 3) by the number of ferrocene sites within a single dendrimer molecule, assuming that all of the ferrocene sites are electrochemically active.<sup>40</sup> Using this approach, the calculated value of  $\Gamma_s$  is  $2.9 \times 10^{-12}$  mol/ $\text{cm}^2$ .

To investigate the generation of an electroactive label by ALP, the Fc-D modified electrode was incubated in a solution of 0.5 mM *p*-APP, as a substrate for ALP. In the presence of ALP, an irreversible peak appeared near  $-0.1$  V vs MSE (Figure 4c), and the peak current increased with incubation time and leveled off

(34) Tokuhisa, H.; Zhao, M.; Baker, L. A.; Phan, V. T.; Dermody, D. L.; Garcia, M. E.; Peez, R. F.; Crooks, R. M.; Mayer, T. M. *J. Am. Chem. Soc.* **1998**, *120*, 4492.  
 (35) (a) Kondo, T.; Horiuchi, S.; Yagi, I.; Ye, S.; Uosaki, K. *J. Am. Chem. Soc.* **1999**, *121*, 391. (b) Popenoe, D. D.; Deinhammer, R. S.; Porter, M. D. *Langmuir* **1992**, *8*, 2521. (c) Ye, S.; Sato, Y.; Uosaki, K. *Langmuir* **1997**, *13*, 3157.

(36) Jordan, C. E.; Frutos, A. G.; Thiel, A. J.; Corn, R. M. *Anal. Chem.* **1997**, *69*, 4939.  
 (37) Sukhorukov, G. B.; Feigin, L. A.; Montrel, M. M.; Sukhorukov, B. I. *Thin Solid Films* **1995**, *259*, 79.  
 (38) Rosen, I.; Rishpon, J. *J. Electroanal. Chem.* **1989**, *258*, 27.  
 (39) Tang, H. T.; Lunte, C. E.; Halsall, H. B.; Heineman, W. R. *Anal. Chim. Acta* **1988**, *214*, 187.  
 (40) Takada, K.; Diaz, D. J.; Abruña, H. D.; Cuadrado, I.; Casado, C.; Alonso, B.; Morán, M.; Losada, J. *J. Am. Chem. Soc.* **1997**, *119*, 10763.

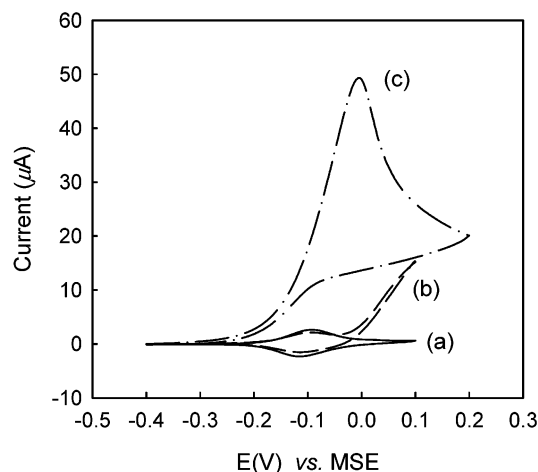
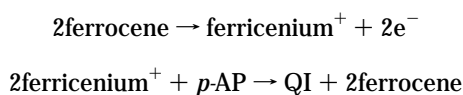


Figure 4. Cyclic voltammogram of (a) Fc-D electrode in EB, the same electrode in a solution of 0.5 mM *p*-APP (b) before and (c) after the addition of ALP. Scan rate of 50 mV/s.

after 30 min. In contrast, such a peak was not observed in the absence of ALP (Figure 4b). These results indicate indirectly that the enzymatic reaction amplifies the generation of electrochemically active molecules, presumably *p*-AP.<sup>26a</sup> It is noted that the anodic peak potential positively shifts from the oxidation potential of *p*-AP (−0.4 V vs MSE) to the oxidation potential of the dendrimetric ferrocenyl groups (−0.1 V vs MSE). The positive shift of potential can be explained by the following mechanism,



where QI (quinoimide) is a molecule of *p*-AP that has been oxidized by loss of two electrons. When the potential scan is reversed, no cathodic peak corresponding to reduction of QI was observed even in an extended negative potential sweep to −0.8 V. The oxidation reaction is thermodynamically favorable, because the surface-immobilized ferricenium is capable of oxidizing solution-phase *p*-AP via a two-step mechanism. The reverse reaction, however, does not occur, because it involves the thermodynamically unfavorable electron transfer from ferrocene to QI. The absence of a cathodic peak for QI reduction and the positive shift of the anodic peak for *p*-AP oxidation strongly suggest that *p*-AP oxidation is occurring via the proposed redox reaction involving ferrocene. Features similar to the irreversible current reported here have been described in other studies.<sup>30,41</sup> Such electrocatalytic reactions are expected to effectively enhance the electric signal for DNA hybridization detection, such as an effect observed by other groups.<sup>8,14,42</sup>

To demonstrate the electronic mediation of Fc-D, the same experiment was conducted with an electrode modified with only PAMAM dendrimers. As shown in Figure 5b, instead of the increase of anodic current due to the electrocatalytic reaction, a broad peak with low current appears at higher positive potential. Although the acid SAM (mixed with MUO) efficiently blocks the

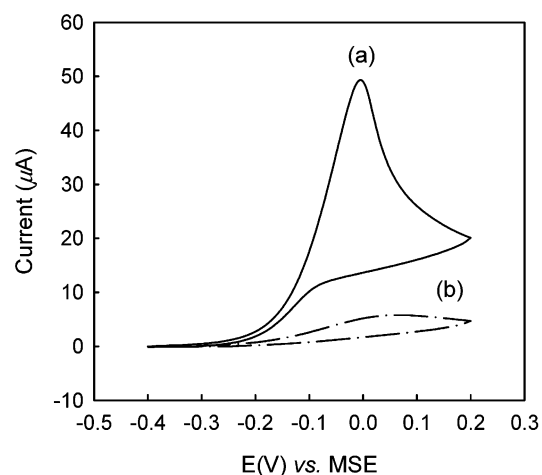


Figure 5. Cyclic voltammogram of (a) Fc-D-modified electrode and (b) PAMAM dendrimer-modified electrode in a solution of 0.5 mM *p*-APP after addition of ALP. Scan rate of 50 mV/s.

most direct electron transfer between *p*-AP and a gold electrode, it is likely that a minor portion of *p*-AP directly oxidizes on the dendrimer modified SAM. We found that gate areas for the direct electron transfer are produced when the dendrimer layer is constructed onto the acid prelayer, which was revealed by the charge-transfer test for  $\text{Fe}(\text{CN})_6^{3-}$ . The gates may be defect sites of gold or dendrimer sites penetrated into the prelayer. Crooks et al. reported that only a dendrimer layer on a gold cannot efficiently block the access of  $\text{Fe}(\text{CN})_6^{3-}$ .<sup>34</sup> Their observation might be also responsible for the direct electron transfer of *p*-AP. Hence, although plenty of electroactive labels (*p*-AP) are generated by the hydrolysis reaction of ALP, the electrochemical signal might not increase in proportion to the amount of biocatalytically generated *p*-AP, because the electron transfer between *p*-AP and the electrode occurs in the limited gates. However, the introduction of ferrocene into the PAMAM-dendrimer solves this problem, leading to a great increase in the electrochemical signal, as shown in Figure 5a, and improved discrimination of signals obtained in the absence and presence of ALP.

**Detection of Sequence-Selective Hybridization by Sandwich-Type Enzyme-Linked Electrochemical DNA Sensor.** In this study, two important factors were applied to an electrochemical DNA assay system, namely, ALP as an electroactive label generator and Fc-D layer as an electrocatalyst to enhance the electrochemical signal via electrocatalytic reaction. According to the processes shown in Scheme 1, a sandwich-type enzyme-linked electrochemical DNA sensor was assembled. Figure 6 shows the electrochemical signals resulting from the sequence-selective hybridization of various targets with the immobilized capture probe. The anodic peaks seen in Figure 6 result from the electrocatalytic oxidation of *p*-AP generated by Av-ALP, and the magnitude of these peaks indirectly reflects the amount of Av-ALP anchored to the immobilized hybrids. We have designed thiolated capture probes containing poly(ethylene glycol) (PEG) to reduce the nonspecific binding of enzyme. As shown in Figure 6d, only the current due to the redox reaction of ferrocene was observed when the electrode was first modified by the capture probe alone and then incubated into a solution of Av-ALP (without the hybridization process of the target and detection probe). However, when we used capture probes lacking PEG, a higher

(41) Alleman, K. S.; Weber, K.; Creager, S. E. *J. Phys. Chem.* **1996**, *100*, 17050.

(42) Kelley, S. O.; Boon, E. M.; Barton, J. K.; Jackson, N. M.; Hill, M. G. *Nucleic Acids Res.* **1999**, *27*, 4830.



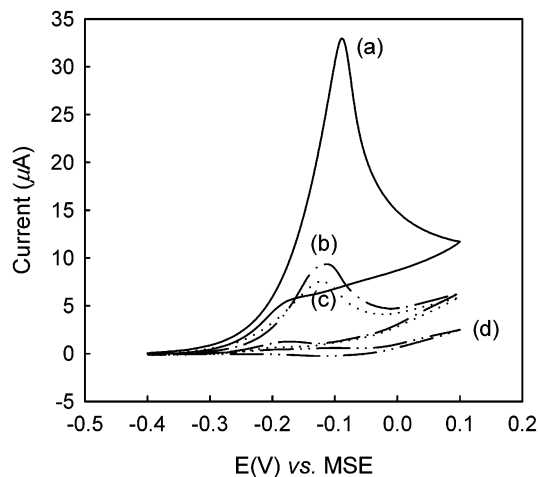


Figure 6. Cyclic voltammogram of enzyme-linked electrodes in a solution of 0.5 mM *p*-APP; scan rate of 50 mV/s in the case of hybridization with (a) 1  $\mu$ M complementary target (T1), (b) 1  $\mu$ M single-base-mismatched target (T3), (c) 1  $\mu$ M noncomplementary target (T2), and (d) without hybridization with target and detection probe.

anodic current was measured (not shown). This result implies that the PEG within the capture probe effectively resists the nonspecific binding of protein to the modified electrode.<sup>43,44</sup>

Figure 6a and c shows the evident difference in electrochemical signals between the complementary (T1) and noncomplementary target DNA (T2). For the hybridization with T1, a sharp increase of 33  $\mu$ A in the oxidation peak current was observed upon addition of *p*-APP (0.5 mM), as shown in Figure 6a. However, when T2 was added instead of T1, the anodic peak current upon addition of *p*-APP was lowered to 7.5  $\mu$ A (Figure 6c). When we also performed the electrochemical detection of hybridization with fully mismatched DNA, it was observed that the increase in electrocatalytic current of fully mismatched DNA is similar to that in T2 (data not shown). The minute increase in electrocatalytic current might be attributed to the nonspecific interaction of target oligomer on the Fc-D-modified surface, leading to the hybridization with detection probe and subsequent association with Av-ALP. As a result, the signal-to-noise ratio in the discriminating sequence is 4.4. The density of the complementary target (T1) was estimated as  $3.5 \times 10^{-12}$  mol/cm<sup>2</sup> from a radio-labeling experiment, obtained by comparing the number of photostimulated luminescence (PSL) counts measured on the hybridized surface with 5'-P<sup>32</sup>-labeled target to PSL values obtained from radiolabeled target DNA spots of known concentrations. Compared with the coverage of immobilized capture probe in the previous section, the hybridization efficiency of our assembled multilayers on T1 is estimated to be  $\sim 73\%$ .<sup>45</sup>

We detected an electrochemical signal for the single-base-mismatched target DNA (T3), in which a single mismatched base is located in the middle of the section that binds to capture probe. In Figure 6b, single-base mismatched duplexes are easily distin-

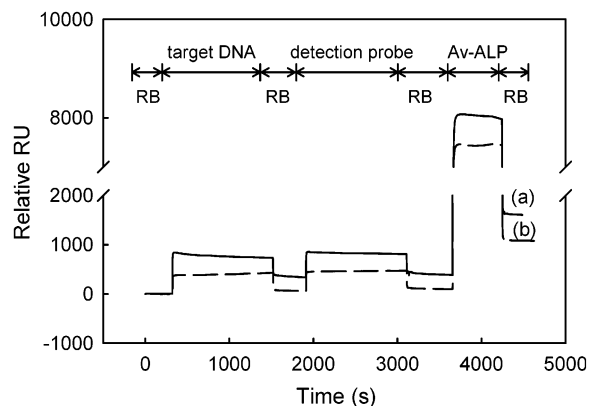


Figure 7. SPR sensograms for the hybridization of target DNAs and detection probe and the subsequent association of Av-ALP onto the capture probe immobilized surface at Fc-D modified electrode. (a) Complementary target DNA (T1) and (b) noncomplementary target DNA (T2). The concentration of target DNA, detection probe, and Av-ALP are the same as the electrochemical experiment. The flow rate was 5  $\mu$ L/min.

guished from complementary duplexes (T1), but they cannot be readily distinguished from noncomplementary duplexes (T2), because the difference between T2 and T3 is trivial, assuming that the T2 signal is wholly due to its nonspecific binding and the T3 signal contains the same amount of nonspecificity. Nonetheless, it is noted that the target DNA can be detected with good selectivity as well as good sensitivity using our new electrochemical DNA assay.

The hybridization of the target oligonucleotides and detection probe and the subsequent association of Av-ALP were also investigated using in-situ SPR, as shown in Figure 7. To compare with the results obtained by electrochemical measurement, SPR experiments were also carried out using T1 and T2. Upon exposure of the capture-probe-coated Fc-D-modified electrode to a solution of T1 or T2, the SPR signal of T1 is nearly 6 times greater than that of T2 (see Figure 7). However, the signal difference between the two targets decreased after the subsequent injection of biotinylated detection probe and Av-ALP. As a result, the final differential ratio of SPR signal between T1 and T2 was 1.5, which is much smaller than the value of 4.4 obtained electrochemically. According to the electrochemical impedance data for DNA sensor assembly reported in Willner's paper,<sup>17a</sup> the electron-transfer resistance of mutant DNA was more than double that of normal DNA upon the association with avidin-alkaline phosphatase. However, the increase in resistance due to the enzymatic reaction, which results in biocatalyzed precipitation of substrate, led to a 4-fold improvement in the hybridization detection signal, indicating the enzymatic reaction is a very efficient amplifier of the detection signal. We think that in our system the Av-ALP amplifies the generation of electroactive label (*p*-AP) via enzymatic reaction and in addition the Fc-D layer enhances the electrochemical oxidation signal, since electrochemically generated ferricenium is reduced back to ferrocene by *p*-AP species.

Our electrochemical detection method is suitable not only for DNA assays, including single-base mismatched target; it should also prove useful for the quantification of target hybridization on the basis of electrocatalytic current. Figure 8 shows the calibration

(43) (a) Yousaf, M. N.; Mrksich, M. *J. Am. Chem. Soc.* **1999**, *121*, 4286. (b) Houseman, B. T.; Huh, J. H.; Kron, S. J.; Mrksich, M. *Nat. Biotechnol.* **2002**, *20*, 270.

(44) Lahiri, J.; Isaacs, L.; Tien, J.; Whitesides, G. M. *Anal. Chem.* **1999**, *71*, 777.

(45) (a) Herne, T. M.; Tarlov, M. *J. Am. Chem. Soc.* **1997**, *119*, 8916. (b) Boncheva, M.; Scheibler, L.; Lincoln, P.; Vogel, H.; Åkerman, B. *Langmuir* **1999**, *15*, 4317.

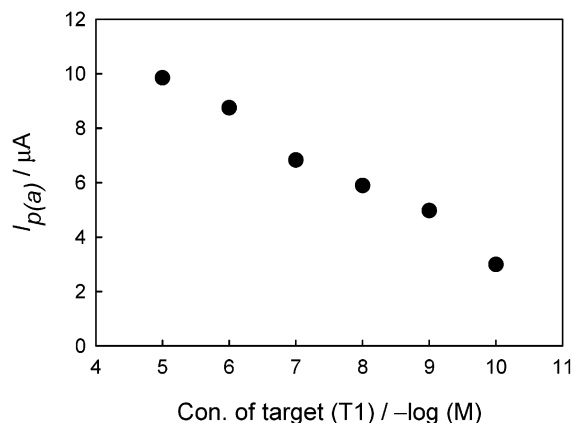


Figure 8. Calibration plot corresponding to changes in anodic peak current upon different concentrations of complementary target DNA (T1) from 0.1 nM to 10  $\mu\text{M}$  after incubation in a solution containing 0.5 mM *p*-APP for 1 min at a scan rate of 50 mV/s.

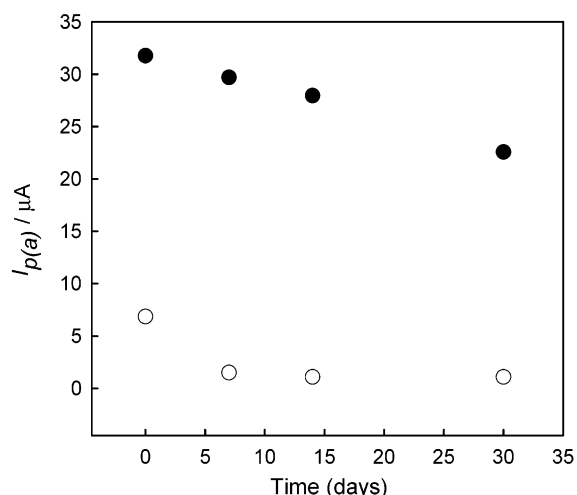


Figure 9. Plot of anodic peak currents to storage time. The change for anodic peak current of an enzyme-linked DNA sensor is measured in a solution of 0.5 mM *p*-APP solution at 50 mV/s for 30 days. (●), complementary target DNA (T1); (○), noncomplementary target DNA (T2).

plot for the change in electrocatalytic peak current as a function of target (T1) concentration. The immobilized capture probe was allowed to hybridize with each target DNA (T1) at different concentrations, followed by hybridization with the detection probe and association with Av-ALP. The catalytic current was then measured immediately after addition of a solution of 0.5 mM *p*-APP. Figure 8 shows that the hybridization signal ( $I_{p(a)}$ ) increases with the target concentration over the concentration range of 0.1 nM to 10  $\mu\text{M}$ . Since the current of negative control is  $\sim 1.2 \mu\text{A}$  measured at 1 min after the addition of T2, the target DNA can be analyzed at a detection limit of 0.1 nM (20 fmol) ( $S/N > 3.0$ ).

As a control experiment, the electrochemical signals of non-complementary and single-base-mismatched targets were monitored as a function of target concentration in the same way. Although a minute electrocatalytic current, which is attributed to the nonspecific adsorption of Av-ALP to the sensing interface, was observed in both cases, the linear response to concentration observed with the complementary target was not observed.

**Long-Term Stability.** The long-term stability of the enzyme label was also examined by measuring the electrochemical response of the enzyme-linked DNA assay electrode over a period of 30 days, storing the same electrode in 0.05 M Tris buffer solution (pH 7.4) at 4  $^{\circ}\text{C}$ . After 5 days, although the electrochemical response only decreased by 6.5% for T1, the response of T2 was lowered by 78%. In fact, the response current was found to decline gradually over the 30 days as shown in Figure 9. It seems very likely that the gradual fall in the response current was due to a gradual deactivation of attached ALP after repeated experiments on the same electrode.

## CONCLUSIONS

We have developed a new sandwich-type electrochemical DNA sensor using an Fc-D conjugates-mediated electrocatalytic reaction of an electroactive label generated biocatalytically by ALP. By comparison with SPR and CV results, we demonstrated that electrocatalysis enhanced the ability to discriminate between DNA sequences. A new combination of electrocatalysis using Fc-D and biochemical amplification with ALP enabled the sequence-selective detection of various targets, including single-base mismatched oligonucleotide, and also the quantification of target over a range of concentrations (0.1 nM to 10  $\mu\text{M}$ ). These results suggest that the introduction of the electroactive layer will allow highly sensitive amperometric measurements of ALP label in EEIA, as well as DNA biosensors. This approach may also be useful as a new electrochemical detection method for the recognition of various proteins using ALP labels in protein arrays.

## ACKNOWLEDGMENT

J. Kwak gratefully acknowledges support from the Korean Ministry of Science and Technology through National R&D Project for Nano Science and Technology. In addition, we gratefully acknowledge support in part from Brain Korea 21, MICROS, and IMT 2000 projects. The authors thank Prof. Hak-Sung Kim (KAIST) for the SPR measurements and Prof. Insung S. Choi (KAIST) for support regarding the FT-IR measurements.

Received for review March 12, 2003. Accepted August 6, 2003.

AC034253X